# Lightwave Switching in Semiconductor Microring Devices by Free Carrier Injection

Tarek A. Ibrahim, *Student Member, IEEE*, W. Cao, Y. Kim, J. Li, J. Goldhar, P.-T. Ho, and Chi H. Lee, *Fellow, IEEE, Fellow, OSA*

***Abstract*—Using a conventional microwave photonic technique, we demonstrate lightwave switching in laterally coupled GaAs–AlGaAs microring resonators by free carrier injection. The ring waveguide is optically pumped just above its bandgap energy, which results in a temporal tuning of the microring resonant wavelengths by the refractive index change due to the induced free carriers. Both the transmission and the phase function of the resonators are investigated and used to demonstrate all-optical switching. The switching time, limited by surface recombination of carriers, is 20 ps. A switching energy of a few picojoules shifts the microring resonance by 1.2 nm.**

***Index Terms*—All-optical switching, carrier injection, microresonators, optical pumping, pump and probe, single photon absorption.**

## I. Introduction

ALL-OPTICAL switching devices operating at the 1.55-$\mu$m wavelength are necessary components for future high-speed optical telecommunication systems. Therefore, the need for a fast, low threshold, compact, and all-optical switch has drastically increased in the last few years. In this regard, semiconductor optical switching devices have been the main focus of the ongoing research because semiconductors have shown large nonlinearities and they can be integrated with other optoelectronic devices such as microlasers and amplifiers. Two main factors would limit the performance of a semiconductor straight waveguide optical switch: carrier lifetime and interaction length [1], [2]. In bulk semiconductors, the carrier lifetime can approach a few nanoseconds and thus limit the switching speed of the device to below 1 GHz. However, in a tightly confined semiconductor waveguide, the carrier lifetime can be as short as tens of picoseconds due to surface recombination. If the phase change achieved by carrier injection is much higher than the change in absorption, then the interaction length of a semiconductor optical waveguide based switch can be reduced if configured into a Mach–Zehnder interferometer. In such a case, the phase shift required to switch from on to off or vice versa is exactly $\pi$ rad. Moreover, if the waveguide is formed into a ring structure, the amount of phase shift required for switching is drastically reduced because the interaction length of the device is effectively enhanced by the finesse of the microring cavity [3].

Manuscript received April 24, 2003; revised September 24, 2003.

The authors are with the Laboratory for Physical Sciences, College Park, MD 20740 USA and the Department of Electrical and Computer Engineering, University of Maryland, College Park, MD 20742 USA (e-mail: tadly@lps.umd.edu).

Digital Object Identifier 10.1109/JLT.2003.819800

One way to use the microring resonator as an all-optical switch was demonstrated in [4], in which the pump beam was tuned to one of the microring resonances to switch a probe beam tuned to the next higher resonance. Since the pump beam energy was just above half the bandgap of the material, two-photon absorption (TPA) was the nonlinear process responsible for switching. The switching speed was limited by the photon lifetime as well as the carrier recombination lifetime.

Nonlinear optical phenomena can be induced in semiconductors more efficiently by free carrier injection induced by single photon absorption (SPA). By optically pumping the semiconductor material with photon radiation above its bandgap energy, each absorbed photon generates an electron-hole pair. These injected carriers change the gain-loss coefficient and the refractive index of the semiconductor material. The optoelectronics technique for free carrier injection has become a conventional microwave photonic method for optically controlled microwave devices [5]. In this manner, millimeter-wave propagation in a semiconductor waveguide had been controlled by an optical signal [6], [7]. This mechanism offers some advantages in comparison with what has been previously demonstrated using TPA.

1) The pump beam does not need to be tuned to one of the microring resonance wavelengths.
2) The switching speed is no longer limited by the cavity charging time since the pump beam does not resonate in the microring, allowing ultrafast switching to take place.
3) The absorption mechanism is much more efficient.
4) With proper pump beam spot size and wavelength, switching power can be much smaller.

On the other hand, TPA might be desirable for in-plane all-optical signal processing. In [8], tuning of a microdisk resonator filter was demonstrated by carrier injection through an electrical current.

In this paper, we demonstrate all-optical switching in laterally coupled GaAs–AlGaAs microring resonators by optical pumping near the material bandgap energy. We investigate the use of both the transmission and phase transfer functions of the ring resonator for nonlinear switching.

## II. Transmission Switching

### A. Theory

The electric field circulating inside the microring resonator shown in Fig. 1(a) can be written as

$$E_1(t) = -j\kappa_1 E_0 + r_1 r_2 a E_1(t-\tau)e^{j\phi} \tag{1}$$

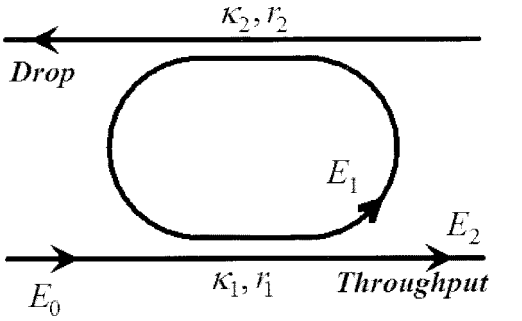


(a)

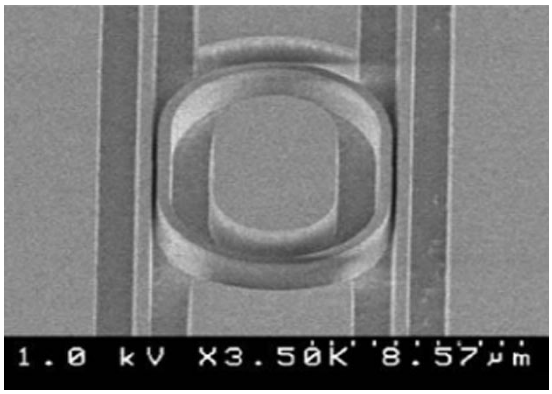


(b)

Fig. 1. (a) Schematic diagram and (b) SEM picture of the microring resonator.

where $E_0$ is the input continuous-wave (CW) probe beam, $r_1$ and $r_2$ are the field transmission coefficients at the input and output waveguides, respectively, $a$ is the field round-trip loss, $\kappa_1$ is the field coupling coefficient between the input waveguide and the ring waveguide such that $\kappa_1^2 + r_1^2 = 1$, and $\tau$ is the round-trip time of the resonator. The resonator round-trip phase $\phi$ is given by

$$\phi = \frac{2\pi}{\lambda} nL \tag{2}$$

where $\lambda$ is the probe beam wavelength, $n$ is the refractive index of the ring waveguide, which is a function of carrier density, and $L$ is the circumference of the ring resonator.

At steady state, the transmission-transfer function of the resonator is given by

$$\frac{E_2}{E_0} = \frac{r_1 - a r_2 e^{j\phi}}{1 - a r_1 r_2 e^{j\phi}}. \tag{3}$$

Equation (3) suggests that the ring cavity is very similar to a Fabry–Pérot cavity, with the embedded advantage of the multiple input–output ports due to the ring geometry. Near resonance, the transfer function of the ring resonator given by (3) is nonlinear with respect to $\phi$, and thus can be used for switching, thresholding, and reshaping.

The dynamic behavior of the circulating electric field can be simulated by numerically solving (1) after substituting from (2).

The first device used in the experiment is a single race track laterally coupled to two straight waveguide buses with a straight coupling section of 10 $\mu$m, as shown in Fig. 1(b) [9]. Fig. 2 shows the measured spectral response of the microresonator at

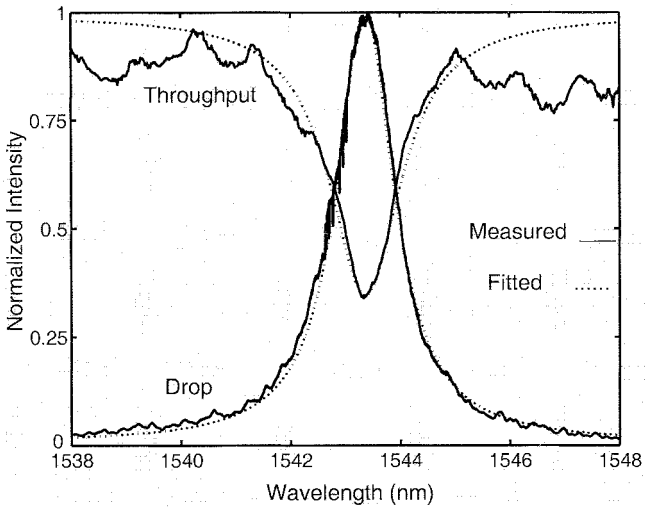


Fig. 2. Measured (solid lines) and fitted (dotted lines) spectral response at the throughput and drop ports of the microring resonator around 1543.4 nm. The discrepancy between the measured and fitted throughput spectrums is due to the resonances of the Fabry–Pérot cavity formed by the cleaved facets of the throughput waveguide.

both the throughput and drop ports at its TE resonance mode at 1543.4 nm. The microring linear parameters could be extracted by fitting both the throughput and drop port spectral responses with the assumption of symmetrical couplings at the input and output waveguides. The round-trip power loss is 24% and the coupling coefficient is 11%. The ring has a 3-dB bandwidth of 1.3 nm, an intrinsic quality factor of 1200, a free spectral range of 18 nm, and a finesse of 14.

### *B. Experiment*

All-optical switching is accomplished using the pump-probe scheme, in which a high-intensity pump pulse is used to control the transmission of a CW probe beam tuned to one of the microring resonances. By sweeping the probe beam wavelength across the microring resonance and detecting the time variation of the dropped signal, the resonance wavelength shift of the microring and hence its refractive index change can be measured.

The experimental setup is as follows. The pump beam is a train of model-locked Ti: Sapphire pulses at 800 nm. The pulse width is typically 100 fs with 1-kHz repetition rate. The average power of the beam is attenuated to less than 1 $\mu$W at the device surface. A lens system is used to focus the beam to about 50-$\mu$m spot size and to pump the microring from top. The probe beam is provided by an external cavity semiconductor laser diode, which is tunable around 1550 nm. The laser diode is tuned to the microring resonance wavelength at 1543.4 nm with an average power of a few milliwatts. The probe beam is fed into the input port of the resonator using a conically tipped fiber. The insertion loss is typically 7 dB per facet. The output of the drop port is also collected with another conically tipped fiber, optically amplified, fed to a 40-GHz detector, and monitored by a 50-GHz scope.

Since the bandgap wavelength of GaAs is around 800 nm, the pump pulse is almost fully absorbed in the microring waveguide and high-density free carriers are generated. These car-

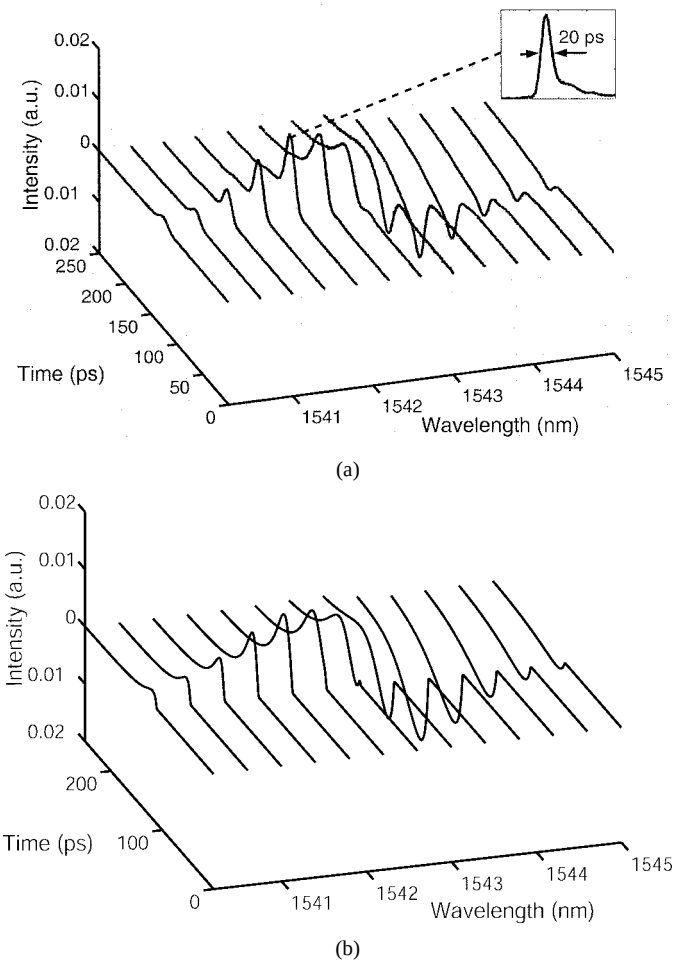


Fig. 3. (a) Measured and (b) simulated modulation of the dropped signal for different input probe beam wavelength (DC level has been removed in both (a) and (b) for clarity).

riers decrease the refractive index of the microring waveguide and cause a temporarily blue shift of the microring resonance wavelength. When the free carriers diffuse to the waveguide walls and recombine, the effect diminishes. If a probe beam is tuned to one of these microring resonant wavelengths, the output probe signal will be modulated. The depth of modulation depends on the magnitude of the resonance-wavelength shift. In addition, the steeper the resonator profile, or, in other words, the higher the cavity finesse, the larger the modulation of the output signal for a given wavelength shift.

Fig. 3(a) shows a three-dimensional plot of the time variation of the dropped probe signal versus its wavelength. When the probe beam was initially tuned to the shorter wavelength side of the microring resonant wavelength, the carrier-induced blue shift in the resonance brought the probe beam into resonance and was temporarily dropped at the output; thus it experienced a rapid increase in transmission. When the probe beam was initially tuned to the resonant wavelength, the carrier-induced index change shifted the resonance away from the probe beam, resulting in a rapid attenuation of the dropped signal. Simulation results shown in Fig. 3(b) are in good agreement with measured data.

By measuring the switching contrast of the dropped beam at the different probe wavelengths, one can deduce the amount of resonance wavelength shift. Our simulation model yields a maximum refractive index change of $2.6 \times 10^{-3}$ that leads to a resonance wavelength shift of 1.2 nm. The switching contrast is approximately 7 dB. Higher switching contrast can be obtained by injecting more carriers or by using a critically coupled resonator [10]. A rise time of 10 ps is measured for the dropped probe beam and is limited by the detection system. A switching window of 20 ps is obtained and shown in Fig. 3(a).

### C. Discussion

When carriers are injected into a GaAs waveguide, its refractive index has the following expression [6]:

$$\eta, k = \frac{1}{2}\left\{\pm\left(\varepsilon_L - \frac{\omega_p^2}{\omega^2+\nu^2}\right) + \left[\left(\varepsilon_L - \frac{\omega_p^2}{\omega^2+\nu^2}\right)^2 + \left(\frac{\nu}{\omega}\frac{\omega_p^2}{\omega^2+\nu^2}\right)^2\right]^{\frac{1}{2}}\right\}^{\frac{1}{2}} \quad (4)$$

in which $\eta$ and $k$, the real and imaginary parts of the complex refractive index, are obtained by selecting the "+" or "−" sign of the leading term on the right-hand side of (4), respectively. Equation (4) shows that the refractive index depends on the dielectric constant of the material $\varepsilon_L$, the plasma frequency $\omega_p$, the collision frequency of the carriers $\nu$, and the frequency of the propagating probe beam $\omega$. The plasma frequency is given by

$$\omega_p^2 = \frac{n_p e^2}{\varepsilon_0 m^*} \quad (5)$$

where $n_p$ is the free carrier density, $e$ is the free electron charge, $\varepsilon_0$ is the free-space permittivity, and $m^*$ is the effective mass of the carrier.

The effective pump energy that hits the microring is 20 pJ/pulse, and this corresponds to $8 \times 10^7$ photons/pulse. Since the absorption coefficient of GaAs at 800 nm is $10^4$ cm$^{-1}$, a carrier density of $2.5 \times 10^{18}$ cm$^{-3}$ is expected. In Fig. 4(a), we plot (4), and in Fig. 4(b), we plot the real part of refractive index change versus the injected free carrier density at a probe beam wavelength of 1543.4 nm. For a carrier density of $2.5 \times 10^{18}$ cm$^{-3}$, a refractive index change of $3 \times 10^{-3}$ is estimated, which is consistent with the value obtained from the experiment. Fig. 4(a) shows that the change in the imaginary part of the refractive index at that value of carrier density is on the order of $10^{-5}$. Thus the additional loss due to the free carriers can be neglected.

To study the polarization dependence of the optical pump signal used for switching, we adjusted the polarization of the pump beam to the two perpendicular linear polarizations with respect to the device geometry. Negligible polarization sensitivity was measured, which is another advantage of the SPA technique in comparison to the TPA. In the TPA case, proper polarization of the pump beam has to be taken care of to match that of the microring device. This is mainly because of birefringence in the microring waveguide, which results in a splitting between the TE and TM modes. Another aspect to be addressed here is the pump signal wavelength. TPA requires that the pump

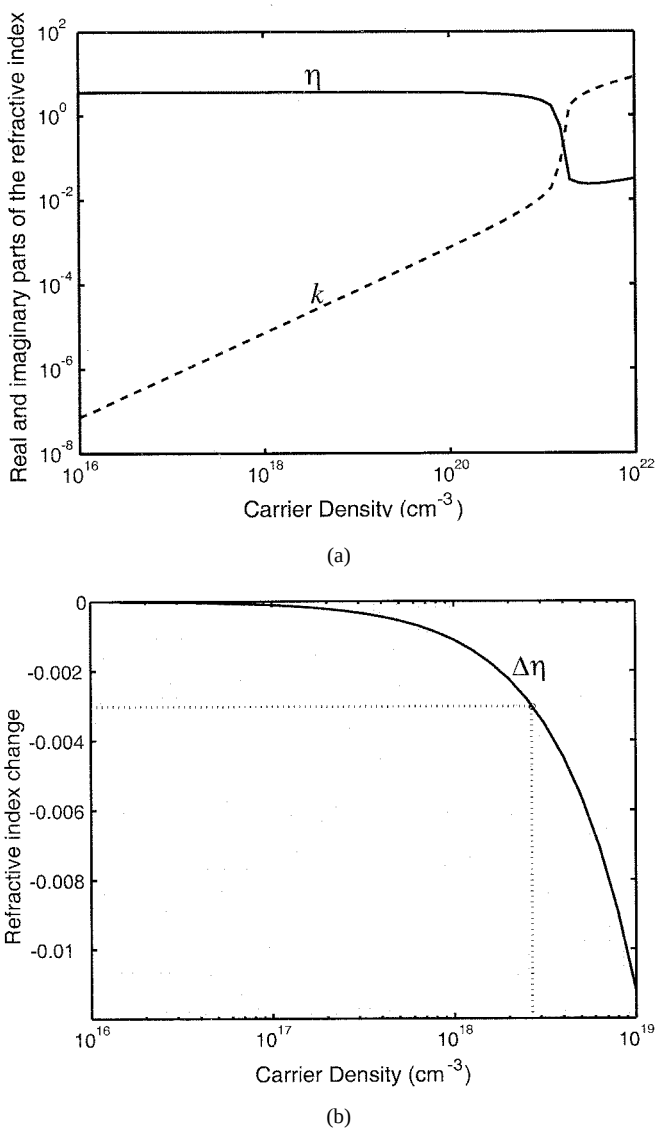


Fig. 4. (a) Real (solid) and imaginary (dotted) parts of the refractive index and (b) real part of the refractive index change versus carrier density for the microring GaAs waveguide at the probe wavelength.

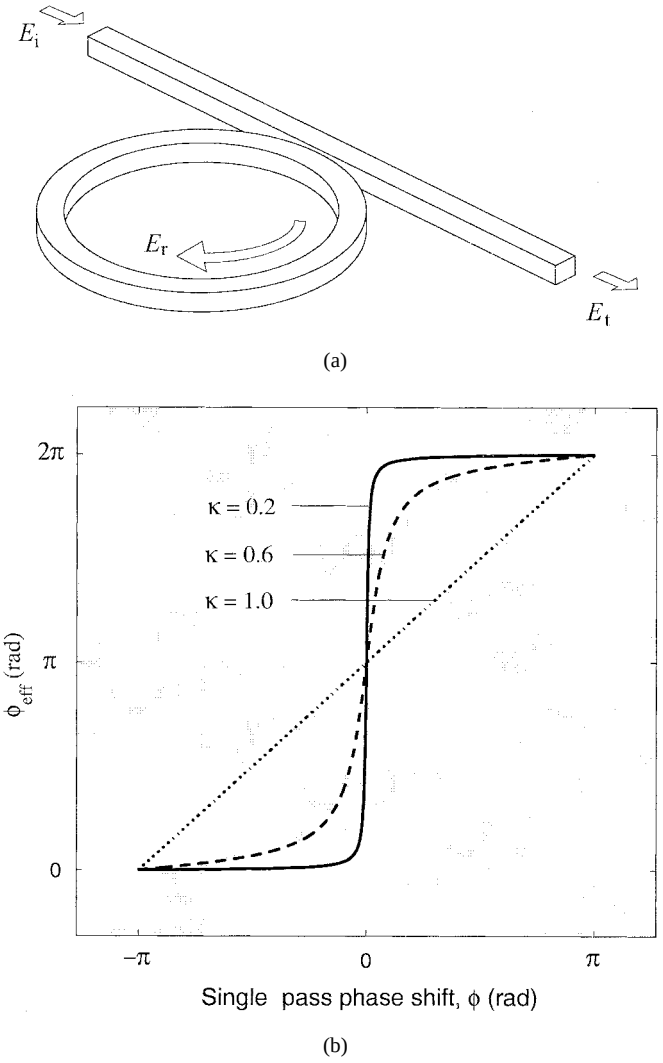


Fig. 5. (a) Schematic diagram of a ring resonator coupled to a straight waveguide and (b) phase enhancement of a lossless resonator for different coupling coefficient $\kappa$.

beam signal be tuned exactly to the microring resonance wavelength. This restricts the switching speed of the device to that of the device bandwidth. Moreover, as the resonance is tuned by the presence of the pump signal, the pump signal itself becomes out of resonance and the dynamic performance of the device is degraded. SPA mechanism does not suffer from the above disadvantage because the pump beam wavelength is not tuned to the device resonance, which allows ultrafast switching to take place and gives more flexibility in terms of the pump source wavelength.

## III. Phase Switching

So far we have only discussed the use of the transmission-transfer function of the microring resonator for switching. However, an examination of its phase-transfer function reveals a similar nonlinear enhancement. A microring coupled to a single waveguide, as shown in Fig. 5(a), forms a phase filter. The phase shift of a signal after passing through the ring is given by [11]

$$\phi_{eff} = \pi + \phi + \tan^{-1}\frac{r\sin\phi}{a - r\cos\phi} + \tan^{-1}\frac{ar\sin\phi}{1 - ar\cos\phi} \quad (6)$$

where $r$ is the field transmission coefficient and $\phi$ is the round-trip phase of the resonator, defined by (2). In Fig. 5(b), we plot (6) for different values of the field coupling coefficient $\kappa = (1 - r^2)^{1/2}$ for a lossless resonator $(a = 1)$. Near resonance $(\phi \approx 0)$, the slope of the effective phase becomes very steep, and hence the device output phase is very sensitive to changes in the single-pass phase shift of the microring. This phase enhancement can be observed by introducing the microring resonator into one arm of a Mach–Zehnder interferometer (MZI). Although an MZI requires a $\pi$ phase shift for switching, Fig. 5(b) shows that such an amount of phase shift can be obtained with a drastically reduced single-pass phase shift of a microring resonator introduced on one arm of the MZI. In other words, the amount of index change required to switch the MZI is dramatically reduced. It is worth

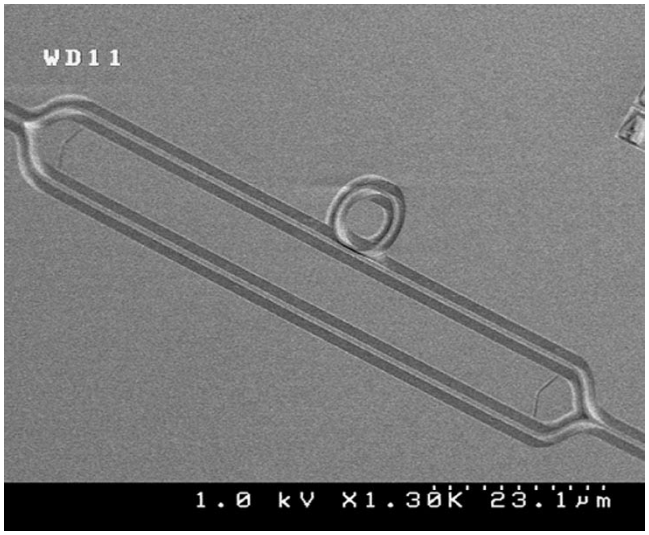


Fig. 6. SEM picture of the MZI loaded with a microring resonator device.

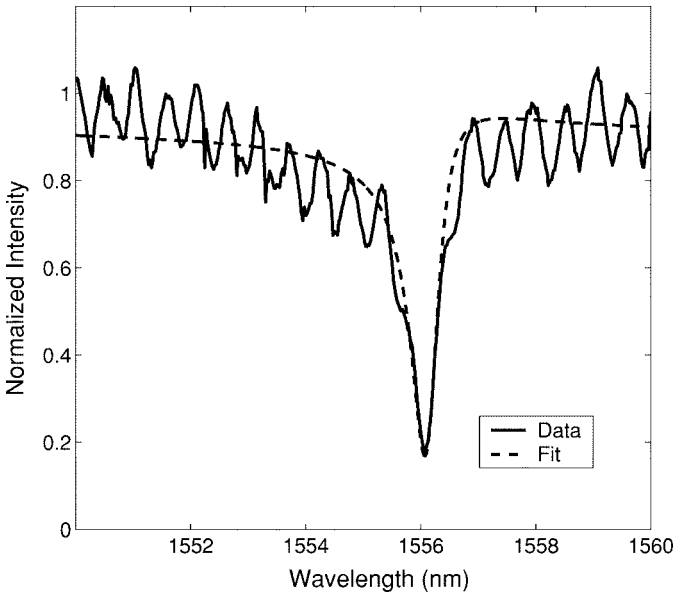


Fig. 7. Measured (solid line) and fitted (dashed line) spectral response of the MZI loaded ring device around its resonance wavelength at 1556 nm. The ringing in the measured spectrum is due to the high reflectivity of the uncoated input and output cleaved facets of the device, which acts as a Fabry–Pérot cavity.

mentioning here that the propagation loss of the microring has to be minimum for high interference visibility between the two arms of the MZI and hence efficient switching. Fig. 6 shows a scanning electron microscope (SEM) picture of an MZI loaded with a microring resonator. The spectral response of the device is shown in Fig. 7. The device has an intrinsic quality factor of 2060 and an estimated finesse of 18.

We used the same experimental setup mentioned earlier to pump the device from top. In Fig. 8, we plot the OFF–ON switching behavior of the device, when the probe beam was initially tuned to the microring resonance at 1556 nm. A switching window of 24 ps is obtained, allowing 40-GHz data processing. An effective energy of 4 pJ/pulse is used to switch the device, which is one order of magnitude less than that required by TPA [4].

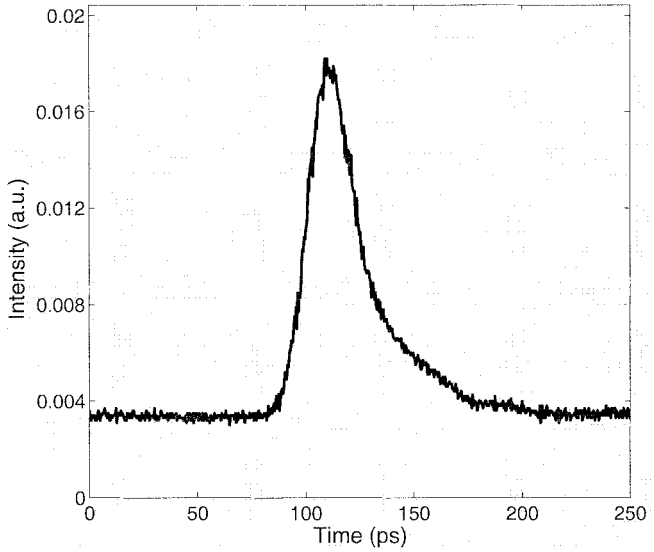


Fig. 8. The off–on switching behavior of the MZI loaded ring device when the probe beam was initially tuned to the microring resonance at 1556 nm.

## IV. Carrier Lifetime

The speed of these devices is mainly limited by the carrier lifetime of the guiding material. To measure the carrier lifetime independently, we optically pumped a tapered straight waveguide at different width sections. We increased the pumping energy so that enough carriers were injected into the waveguide and absorption was observed in a probe beam. By detecting the intensity variation of the probe beam, we could measure the recovery time of the transmitted signal and hence the carrier lifetime. In a tightly confined waveguide, diffusion to the waveguide walls dominates, where fast surface recombination occurs. In Fig. 9(a), we plot the normalized transmitted probe intensity when the waveguide was pumped at different cross-sections; and in Fig. 9(b), we plot the carrier lifetime versus the its diffusion length, which is approximately half the waveguide width. As can be seen, the carrier lifetime varies quadratically with the diffusion length as expected due to the diffusion processes. Since the guiding layer is made of intrinsic bulk material, ambipolar diffusion takes action where both electrons and holes contribute to the diffusion process. Using the Einstein relation, we fitted the carrier lifetime curve and extracted the ambipolar diffusion constant to be 19.2 $cm^2/s$. The ambipolar diffusion constant calculated from published values of electron and hole mobilities and diffusion constants of GaAs [12] is found to be 19.4 $cm^2/s$, which is very close to the measured value. Faster response time can be obtained by dc biasing the microresonator waveguide, where a static electric field normal to the epitaxial layer is induced and rapidly sweeps the free carriers out of the waveguide core [13].

## V. Conclusion

In summary, we have demonstrated all-optical switching by carrier injection induced by SPA in laterally coupled GaAs–AlGaAs microring resonators. Simulation results have been shown to be in good agreement with measured data. We investigated both the transmission and phase functions of the resonator using

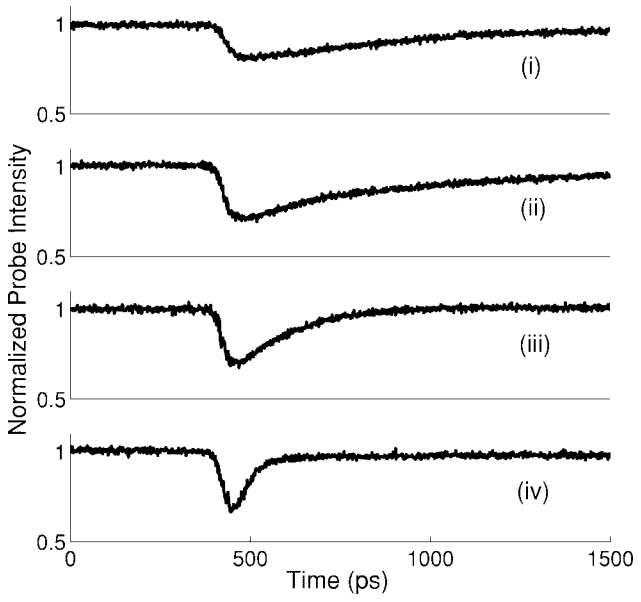


(a)

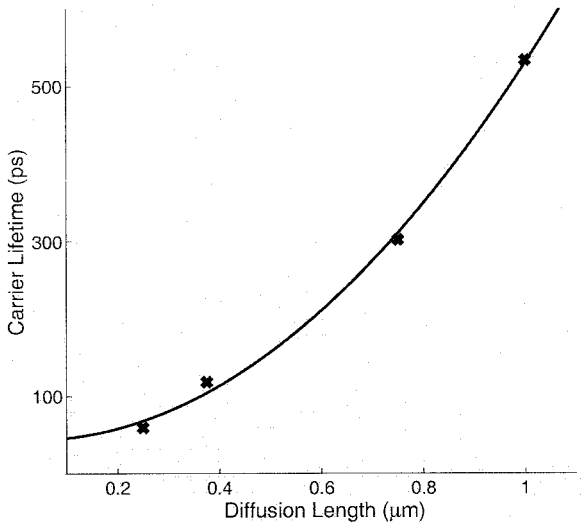


(b)

Fig. 9. (a) Normalized transmitted probe intensity when the tapered straight waveguide was optically pumped at its width of (i) 2.0 $\mu$m, (ii) 1.5 $\mu$m, (iii) 0.8 $\mu$m, and (iv) 0.5 $\mu$m. (b) Measured and fitted carrier lifetime of the GaAs waveguide versus the carrier diffusion length.

two different device configurations. The switching energy is found to be at least one order of magnitude less than that required by TPA. These devices have great potential for switching, routing, multiplexing and demultiplexing, and reshaping. Optical pumping can be accomplished by integrated vertical-cavity surface-emitting lasers underneath the microrings or by an array of laser diodes mounted on top of the microrings. The switching speed is only limited by the carrier lifetime and can be enhanced by dc biasing the microring waveguide to sweep out carriers.

## ACKNOWLEDGMENT

P. Absil and J. Hryniewicz fabricated the microring resonator. Great thanks go to M. Saylors and R. Grover of the University of Maryland for the helpful discussions. The authors would also like to thank the staff of the Laboratory for Physical Sciences for support.

## REFERENCES

[1] S. T. Ho, C. E. Soccolich, M. N. Islam, W. S. Hobson, A. F. J. Levi, and R. E. Slusher, "Large nonlinear phase shifts in low-loss $Al_xGa_{1-x}As$ waveguides near half-gap," *Appl. Phys. Lett.*, vol. 59, pp. 2558–2560, Nov. 1991.

[2] C. Coriasso, D. Campi, C. Cacciatore, L. Faustini, C. Rigo, and A. Stano, "All-optical switching and pulse routing in a distributed-feedback waveguide device," *Opt. Lett.*, vol. 23, pp. 183–185, Feb. 1998.

[3] S. Blair, J. E. Heebner, and R. W. Boyd, "Beyond the absorption-limited nonlinear phase shift with microring resonators," *Opt. Lett.*, vol. 27, pp. 357–359, Mar. 2002.

[4] V. Van, T. A. Ibrahim, K. Ritter, P. P. Absil, F. G. Johnson, R. Grover, J. Goldhar, and P.-T. Ho, "All-optical nonlinear switching in GaAs–AlGaAs microring resonators," *IEEE Photon. Technol. Lett.*, vol. 14, pp. 74–76, Jan. 2002.

[5] C. H. Lee, *Picosecond Optoelectronic Devices*. London, U.K.: Academic, 1984.

[6] C. H. Lee, P. S. Mak, and A. P. DeFonzo, "Optical control of millimeter-wave propagation in dielectric waveguides," *IEEE J. Quantum Electron.*, vol. QE-16, pp. 277–287, Mar. 1980.

[7] A. M. Yurek, C. D. Striffler, and C. H. Lee, "Optoelectronic devices for millimeter waves," in *Infrared and Millimeter Waves*, K. J. Button, Ed. New York: Academic, 1985, vol. 14, ch. 4, pp. 249–290.

[8] K. Djordjev, S.-J. Choi, S.-J. Choi, and P. D. Dapkus, "Microdisk tunable resonant filters and switches," *IEEE Photon. Technol. Lett.*, vol. 14, pp. 828–830, June 2002.

[9] J. V. Hryniewicz, P. P. Absil, B. E. Little, R. A. Wilson, and P.-T. Ho, "Higher order filter response in coupled micro-ring resonators," *IEEE Photon. Technol. Lett.*, vol. 12, pp. 320–322, Mar. 2000.

[10] P. P. Absil, J. V. Hryniewicz, B. E. Little, R. A. Wilson, L. G. Joneckis, and P.-T. Ho, "Compact microring notch filters," *IEEE Photon. Technol. Lett.*, vol. 12, pp. 398–400, Apr. 2000.

[11] J. E. Heebner and R. W. Boyd, "Enhanced all-optical switching by use of a nonlinear fiber ring resonator," *Opt. Lett.*, vol. 24, pp. 847–849, June 1999.

[12] S. M. Sze, *Physics of Semiconductor Devices*, 2nd ed. New York: Wiley, 1981.

[13] M. Yairi and D. Miller, "Equivalence of diffusive conduction and giant ambipolar diffusion," *J. Appl. Phys.*, vol. 91, pp. 4374–4381, Apr. 2002.

**Tarek A. Ibrahim** (S'03) received the B.S. and M.S. degrees in electrical engineering from Cairo University, Giza, Egypt, in 1996 and 1999, respectively. He is currently working toward the Ph.D. degree at the Laboratory for Physical Sciences, University of Maryland, College Park.

In 1997, he joined the National Institute for Laser Enhanced Sciences, Cairo University, as a Research and Teaching Assistant. His research interests are all-optical signal processing using nonlinear semiconductor microring resonators.

Mr. Ibrahim received the University of Maryland Graduate Fellowship in 1999 and the Distinguished Electrical and Computer Engineering Graduate Research Assistantship in 2001.

**W. Cao**, photograph and biography not available at the time of publication.

**Y. Kim**, photograph and biography not available at the time of publication.

**J. Li** received the B.S. and M.S. degrees from Tsinghua University, Beijing, China, in 1993 and 1996, respectively. She is currently working toward the Ph.D. degree in the Department of Electrical and Computer Engineering at the University of Maryland, College Park.

Her current research focuses on the application of ultrafast lasers to study fast dynamic processes in materials such as superconductors, ferroelectrics, and polymer.

**J. Goldhar**, photograph and biography not available at the time of publication.

**P.-T. Ho**, photograph and biography not available at the time of publication.

**Chi H. Lee** (F'91) received the B.S. degree in electrical engineering from National Taiwan University, Taipei, in 1959 and the Ph.D. degree from Harvard University, Cambridge, MA, in 1968.

He has been with the Department of Electrical and Computer Engineering, University of Maryland, College Park, since 1968 and is currently a Professor Emeritus. His research is in the area of ultrafast optoelectronics and in optically controlled millimeter-wave devices and circuits.

Dr. Lee is a Fellow of the Optical Society of America (OSA) and the Photonic Society of Chinese Americans. He was the Chairman of the Technical Committee on Lightwave Technology in the IEEE Microwave Theory and Techniques (MTT) Society, the program Co-Chair of the topical meeting on "Picosecond Electronics and Optoelectronics" in 1985 and 1987, and the General Co-Chair of the International Meeting on "Microwave Photonics" in 1998. He served as Chairman of the Steering Committee of the International Microwave Photonics Meeting for 1999 and the Chairman of the IEEE/Lasers & Electro-Optics Society (LEOS) Technical Committee on Microwave Photonics from 1997 to 2003. He was the General Chair of the IEEE/LEOS Summer Topical Meeting on Photonics Time/Frequency Measurements and Controls, July 14–16, 2003, in Vancouver, BC, Canada.